International Journal of Electrical and Computer Engineering (IJECE)
Vol. 15, No. 3, June 2025, pp. 2556~2566
ISSN: 2088-8708, DOI: 10.11591/ijece.v15i3.pp2556-2566

Impedance matching and power recovery in response to coil misalignment in wireless power transmission

Lunde Ardhenta[1], Ichijo Hodaka[2], Kazuya Yamaguchi[3], Takuya Hirata[2]
[1]Department of Materials and Informatics, Interdisciplinary Graduate School of Agriculture and Engineering, University of Miyazaki, Miyazaki, Japan
[2]Department of Electrical and Electronic Engineering, University of Miyazaki, Miyazaki, Japan
[3]Department of Control Engineering, National Institute of Technology, Nara College, Yamatokoriyama, Japan

Article Info

Article history:

Received Jul 17, 2024
Revised Dec 16, 2024
Accepted Jan 16, 2025

Keywords:

Coils misalignment
Impedance matching
Maximum power transfer
Symbolic optimization
Wireless power transfer

ABSTRACT

The improper alignment of the coils between the transmitter and receiver has a significant impact on wireless power transfer. If designers carefully calculate the parameters of inductance, capacitance, coupling coefficient, and working frequency and precisely implement these parameters into actual components, the system can optimize power transfer. However, it is evident that such a precise realization is often unachievable. This paper proposes a symbolic condition to maintain significant power despite the misalignment of transmitter and receiver coils. These symbolic conditions constrain parameters by simplifying some variables. This matching condition develops in the inequality of coupling coefficient, working frequency and quality factor, which are a crucial reference for maintaining power transfer. This condition is considered an additional one to the well-known impedance matching condition.

Corresponding Author:

Ichijo Hodaka
Department of Electrical and Electronic Engineering, University of Miyazaki
1-1, Gakuen-Kibanadai-Nishi, Miyazaki, 889-2192, Japan
Email: hijhodaka@cc.miyazaki-u.ac.jp

1. INTRODUCTION

The electrical system in every electric device becomes quite complex and has several possible changes in properties when operational conditions change as technology advances. Wireless power transfer (WPT) is innovative and unlike conventional because it delivers power wirelessly from a power supply as a transmitter side to the load as a receiver side. Using the electromagnetic induction principle, the WPT system can eliminate traditional cable connections, providing electrical equipment with excellent safety and flexibility while resisting dynamic environments [1], [2]. This technology is utilized in various practical applications in everyday life, such as electric vehicles [3]–[5], biomedical devices [6], [7], digital household appliances [8], [9], and industrial electricity [10].

In its application, the phenomenon of induction in the form of compensation plays a vital role in providing power. Therefore, based on the pairing configuration of coils and capacitors in each transmitter and receiver side, these systems can be categorized into four types: both sides in series (S-S), series in transmitter-parallel in the receiver (S-P), parallel in transmitter-series in the receiver (P-S), and both sides in parallel (P-P) [11]–[15]. Some more complicated developmental compensation topologies can be formed from these four topologies.

The most important thing to consider is the selection of appropriate compensation for a particular application determined by the transfer properties of the WPT system. Therefore, choosing compensation topology is crucial to evaluate by comparing the influence of different transmission characteristics on the power-transferred. Shevchenko *et al.* [16] has not presented a comprehensive analytical review of the power transfer of each topology, but they have provided suggestions on the values of inductors and capacitors for some topologies.

Dai *et al.* [17] discusses a topology selection method based on robustness, voltage gain, and efficiency, as well as optimizing the parameters. However, they do not explain how the power is transferred in each topology. Sagar *et al.* [18] analyzed the mutual inductance, load, and working frequency in S-S and S-P voltage gain topologies only. Movagharnejad and Mertens [19] stated that S-S and S-P topologies are the two most economical configurations coupled with choosing the source and capacitor frequencies appropriately so that the load and coupling coefficients can vary though deliver maximum efficiency. Detka and Górecki [20] presents the general characteristics of WPT, especially the energy transmission mechanism, discusses its advantages and disadvantages, and also discusses its application in certain industrial fields. Mahesh *et al.* [21] describes several topologies in general without explaining how to choose the correct topology for an application. Rehman *et al.* [22] investigated two basic topologies, S-S and S-P, for unsymmetrical and symmetrical coils and calculated system efficiency. Using fundamental topology, Wang *et al.* [23] proposed a method to evaluate power transfer capability and analyze bifurcation phenomena. Venkatesan *et al.* [24] investigated the basic topology and its development, especially the transmitter side and output characteristics. From this valuable research, topology selection is one of the most challenging aspects of building a WPT system. In order to make a preference of the topology based on the unknown maximum power distribution, we have to compare each topology and its characteristics in terms of power quantity.

In actual conditions, it may not be easy to achieve the maximum power, particularly if the coils for power transfer are not properly aligned. This paper proposes a symbolic impedance matching method to adapt to dynamically moving coils for basic topologies. The proposed method is demonstrated by two parameters that greatly influence the reaching of maximum power transfer: the power supply frequency and a coupling coefficient. The operating frequency can be adjusted more quickly from a technical perspective, and the coupling coefficient represents the coil misalignment in the power transferred of the WPT system. This investigation is intended to provide a comprehensive and straightforward overview of power transfer, given a general comparison of simulation results. This approach is also applied to some topologies in order to deliver maximum power to the load, which is the main objective of the WPT system.

2. METHOD

This research employs a fundamental WPT circuit combined with impedance matching. Impedance matching plays a key role in maximizing power transfer efficiency. It ensures that the input impedance, including the voltage source, aligns with the output impedance, representing the load. Significant power losses can occur without proper impedance matching, decreasing system performance.

2.1. Wireless power transfer

Paired inductors act as the core of the system WPT and are fundamental to wireless power systems. Ampère's law states that the current flow through an inductor generates a magnetic field. It indicates that a stable current induces a stable magnetic field, and a dynamic current induces a dynamic magnetic field. At the same time, the inductor pair will produce a current when varying magnetic flux penetrates the inductor. The basic electrical circuit used in this model comprises two closed loops, as shown in Figure 1. A particular coil has self-inductance L_1 and L_2 combined with mutual inductance M, where this mutual inductance is an inductive coupling that takes into interpretation the character of the coil and the distance between them. R_s is the resistance within a power source, and R_L is the load resistance used in the system. C_1 and C_2 refers to capacitors combined with inductors in series or parallel to create resonance. The power source, E, is an alternating current (AC) supply. The following equation represents the voltages across the inductor and capacitor, respectively.

$$V_{L1} = j\omega L_1 I_{L1} + j\omega M I_{L2}$$
$$V_{L2} = j\omega M I_{L1} + j\omega L_2 I_{L2}$$
$$V_{C1} = \frac{I_{C1}}{j\omega C_2}$$
$$V_{C2} = \frac{I_{C2}}{j\omega C_2}$$

and M is defined as

$$M = k\sqrt{L_1 L_2}$$

In general, the WPT circuit consists of resistors, inductors, capacitors, and voltage sources, which have a simple configuration whose behavior is represented by Kirchhoff's Law (voltage and current) and Ohm's Law. Based on these laws, the equation for each configuration is derived in the following.

2.1.1. Series-series (S-S)

A series-series topology uses two capacitors, which are in series with each coil, as illustrated in Figure 1(a). This topology is the simplest configuration in the basic WPT topology. The current through the transmitter circuit has the same value for each component ($I_{Rs} = I_{C1} = I_{L1}$), and the receiver has the same condition ($I_{RL} = I_{C2} = I_{L2}$). I_{Rs} represents the transmitter loop current, which started from the voltage source through the capacitor and the coil, while I_{RL} has the opposite direction from the transmitter side; it begins from the load to the coil in a counterclockwise direction. Based on these laws, the equation for each phenomenon of series-series topology is derived as.

$$E = R_s I_{Rs} + \frac{1}{j\omega C_1} I_{C1} + j\omega L_1 I_{L1} + j\omega M I_{L2}$$
$$0 = R_L I_{RL} + \frac{1}{j\omega C_2} I_{C2} + j\omega L_2 I_{L2} + j\omega M I_{L1}$$

By separating the equation based on voltage and current, the impedance is obtained as following equation [21].

$$Z = \begin{bmatrix} -\frac{j}{\omega C_1} + j\omega L_1 + R_s & jM\omega \\ jM\omega & -\frac{j}{\omega C_2} + R_L + j\omega L_2 \end{bmatrix}$$

2.1.2. Series-parallel (S-P)

Figure 1(b) shows that the coil in the transmitter is paired with a capacitor as a previous topology, whereas the receiving coil is paired with a capacitor in parallel. This configuration is called a series-parallel topology. On the transmitter side, the current for each component is the same, but on the receiver side, the current is different for each element. The following is the circuit equations.

$$E = R_s I_{Rs} + \frac{1}{j\omega C_1} I_{C1} + j\omega L_1 I_{L1} + j\omega M I_{L2}$$
$$0 = R_L I_{RL} + j\omega L_2 I_{L2} + j\omega M I_{L1}$$
$$I_{RL} = I_{L2} + I_{C2}$$

The impedance Z of series-parallel is,

$$Z = \begin{bmatrix} \frac{j\omega^3 C_2 L_1 L_2 - jM^2\omega^3 C_2 - j\omega L_1}{\omega^2 C_2 L_2 - 1} - \frac{j\omega C_2 L_2}{C_1(\omega^2 C_2 L_2 - 1)} + \frac{i}{\omega C_1(\omega^2 C_2 L_2 - 1)} + R_s & -\frac{jM\omega}{\omega^2 C_2 L_2 - 1} \\ -\frac{jM\omega}{\omega^2 C_2 L_2 - 1} & R_L - \frac{j\omega L_2}{\omega^2 C_2 L_2 - 1} \end{bmatrix}$$

2.1.3. Parallel-series (P-S)

In a parallel-series circuit, illustrated in Figure 1(c), the circuit configuration is opposite to the previous circuit. The current generated from the source will be directly split into the capacitor and inductor. The circuit equations are:

$$E = R_s I_{Rs} + j\omega L_1 I_{L1} + j\omega M I_{L2}$$
$$I_{Rs} = I_{C1} + I_{L1}$$
$$0 = R_L I_{RL} + \frac{1}{j\omega C_2} I_{C2} + j\omega L_2 I_{L2} + j\omega M I_{L1}$$

The impedance Z of parallel-series is,

$$Z = \begin{bmatrix} R_s - \dfrac{j\omega L_1}{\omega^2 C_1 L_1 - 1} & -\dfrac{jM\omega}{\omega^2 C_1 L_1 - 1} \\ -\dfrac{jM\omega}{\omega^2 C_1 L_1 - 1} & \dfrac{j\omega^3 C_1 L_1 L_2 - jM^2\omega^3 C_1 - j\omega L_2}{\omega^2 C_1 L_1 - 1} - \dfrac{j\omega C_1 L_1}{C_2(\omega^2 C_1 L_1 - 1)} + \dfrac{j}{\omega C_2(\omega^2 C_1 L_1 - 1)} + R_L \end{bmatrix}$$

2.1.4. Parallel-parallel (P-P)

The last basic topology that will be observed is parallel-parallel, where the current in each component will be different, but the voltage will be the same in each component. The equations below are derived from the circuit diagram shown in Figure 1(d).

$$E = R_s I_{Rs} + j\omega L_1 I_{L1} + j\omega M I_{L2}$$
$$I_{Rs} = I_{C1} + I_{L1}$$
$$0 = R_L I_{RL} + j\omega L_2 I_{L2} + j\omega M I_{L1}$$
$$I_{RL} = I_{L2} + I_{C2}$$

The impedance Z of parallel-parallel is,

$$Z = \begin{bmatrix} \dfrac{j\omega L_1 + jM^2\omega^3 C_2 + j\omega^3 C_2 L_1 L_2}{A} + R_s & \dfrac{jM\omega}{A} \\ -\dfrac{jM\omega}{B} & \dfrac{j\omega^3 C_1 L_1 L_2 - j\omega L_2 - jM^2\omega^3 C_1}{B} + R_L \end{bmatrix}$$

where,

$$A = \omega^4 C_1 C_2 L_1 L_2 - \omega^2 C_1 L_1 - \omega^2 C_2 L_2 - M^2\omega^4 C_1 C_2 + 1$$
$$B = -\omega^4 C_1 C_2 L_1 L_2 + \omega^2 C_1 L_1 + \omega^2 C_2 L_2 + M^2\omega^4 C_1 C_2 - 1$$

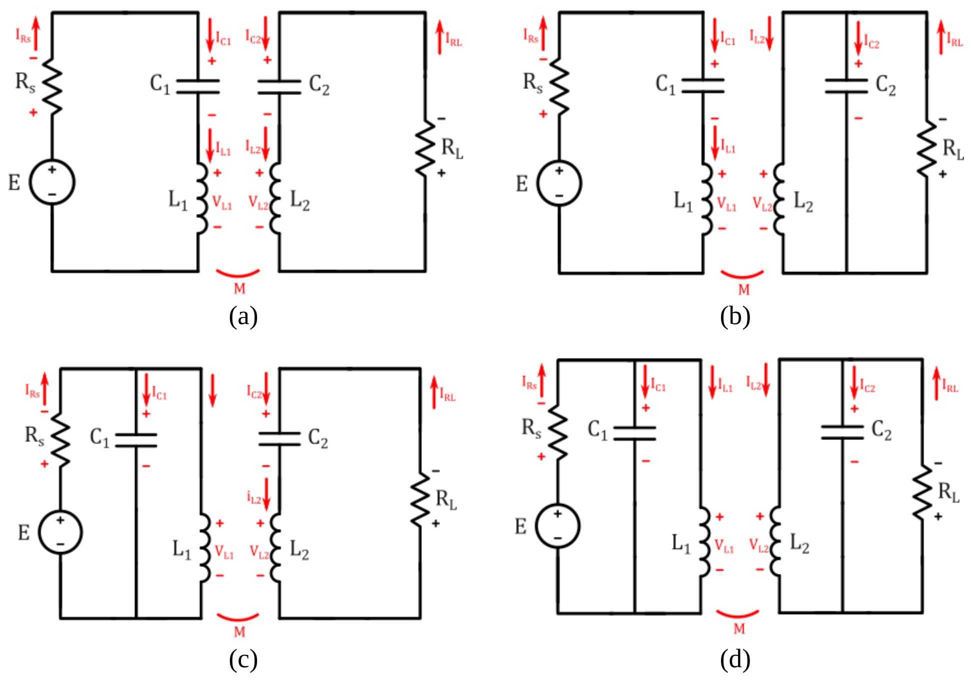

Figure 1. WPT system in (a) series-series topology, (b) series-parallel topology, (c) parallel-series topology, and (d) parallel-parallel topology

2.2. Impedance matching using symbolic condition

Research in WPT primarily focuses on achieving maximum power transfer. One requirement for realizing maximum power transfer is considering system's impedance as a maximum power transfer theorem. Therefore, the impedance between source and load is determined by the impedance matching method in various WPT scenarios. Typically, the impedance matching process in a WPT system covers two parts, as shown in Figure 2. The first part is the power source along with its impedance, while the second is the load's impedance as illustrated in equivalent circuit. Maximum power transfer is obtained when the two parts have the same value or are perfectly matched. The Z_1 is stated as impedance of the input side (voltage source) and the impedance of the load is Z_2, it delivers the maximum power to the load if $Z_1 = \overline{Z_2}$ [23].

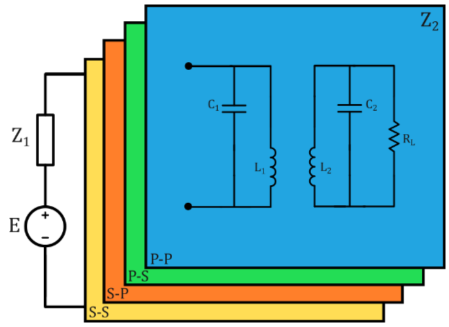

Figure 2. Impedance setting for every topology

The Z_2 impedance is an impedance equation for each topology as in Figure 2, where the Z_1 value must be the same as the conjugate value of Z_2 and Z_1 (the source impedance) is assumed to be a purely resistive load. In order to simplify the calculations and consider the cases of actual conditions where parameters are not always given and kept constant, the following equation is used,

$$Q_1 = \frac{1}{R_s}\sqrt{\frac{L_1}{C_1}},\ Q_2 = \frac{1}{R_L}\sqrt{\frac{L_2}{C_2}},\ \omega_1 = \frac{1}{\sqrt{C_1 L_1}},\ \omega_2 = \frac{1}{\sqrt{C_2 L_2}}$$

The following equations show that the source and load impedance equality are separated into the resistive and reactive components. Table 1 shows two equations for each topology in impedance matching conditions where the value equals 0 and the number of parameters is reduced.

Table 1. Impedance matching condition for each topology

Topology	Impedance matching condition
S-S	$0 = k^2\omega^4 Q_1 Q_2 - \omega^4 Q_1 Q_2 + \omega^2 Q_1 Q_2 \omega_1^2 + \omega^2 Q_1 Q_2 \omega_2^2 - Q_1 Q_2 \omega_1^2 \omega_2^2 - \omega^2 \omega_1 \omega_2$
	$0 = -Q_2 \omega^2 \omega_1 + Q_1 \omega^2 \omega_2 + Q_2 \omega_1 \omega_2^2 - Q_1 \omega_1^2 \omega_2$
S-P	$0 = -k^2\omega^2 Q_1 Q_2 \omega_2 + \omega^2 Q_1 Q_2 \omega_2 - Q_1 Q_2 \omega_1^2 \omega_2 + \omega^2(-\omega_1) + \omega_1 \omega_2^2$
	$0 = -k^2\omega^4 Q_1 + \omega^4 Q_1 - \omega^2 Q_1 \omega_1^2 - \omega^2 Q_1 \omega_2^2 + \omega^2 Q_2 \omega_1 \omega_2 + Q_1 \omega_1^2 \omega_2^2$
P-S	$0 = -k^2\omega^2 Q_1 Q_2 \omega_1 + \omega^2 Q_1 Q_2 \omega_1 - Q_1 Q_2 \omega_1 \omega_2^2 - \omega^2 \omega_2 + \omega_1^2 \omega_2$
	$0 = k^2\omega^4 Q_2 - \omega^4 Q_2 + \omega^2 Q_2 \omega_1^2 + \omega^2 Q_2 \omega_2^2 - \omega^2 Q_1 \omega_1 \omega_2 - Q_2 \omega_1^2 \omega_2^2$
P-P	$0 = -k^2\omega^2 Q_1 Q_2 \omega_1 \omega_2 - k^2\omega^4 + \omega^2 Q_1 Q_2 \omega_1 \omega_2 + \omega^4 - \omega^2 \omega_1^2 - \omega^2 \omega_2^2 + \omega_1^2 \omega_2^2$
	$0 = k^2\omega Q_1 \omega_1 - k^2\omega^2 Q_2 \omega_2 - \omega^2 Q_1 \omega_1 + \omega^2 Q_2 \omega_2 + Q_1 \omega_1 \omega_2^2 - Q_2 \omega_1^2 \omega_2$

3. RESULTS AND DISCUSSION

The wireless power transfer system comprises resistors, inductors, capacitors, and voltage sources. Table 2 shows the notation used in the circuit. In designing a WPT, knowing the values of these parameters is required to fulfill maximum power. This paper aims to help provide considerations for determining the component value based on the impedance matching method.

Based on simplified equation in the previous section, we can simplify the equation by substituting several variables, such as L_1, L_2, C_1, and C_2. Many other papers state that the values of these parameters are determined to be the same to make calculations more straightforward. Still, selecting the component values that are precisely the same would be tough. This paper proposes the specific conditions for the impedance matching condition, which are $Q_1 = Q_2 = Q_0$ and $\omega_1 = \omega_2 = \omega_0$. This equality is arranged to simplify the equation by minimizing the number of variables addressed in the previous section, as shown in Table 3.

When considering the equations as in Table 3 alongside the inequality $0 < k^2 < 1$, which must always physically hold true for the coupling coefficient, it becomes mathematically evident that ω and Q_0 must satisfy the following inequalities. It is understood that in order to maximize power, these parameters must be chosen to fulfill the following inequalities.

Table 2. Notation

Symbol	Representation
E	Voltage source
R_s, R_L	Resistor
C_1, C_2	Capacitor
L_1, L_2	Inductor
V_*	Voltage of component*
I_*	Current of component*
f	Frequency of power supply

Table 3. Proposed equation and selecting condition for four basic topologies

Topology	Proposed equation	Selecting condition
S-S	$0 = k^2\omega^4 Q_0^2 - \omega^4 Q_0^2 + 2\omega^2 Q_0^2\omega_0^2 - Q_0^2\omega_0^4 - \omega^2\omega_0^2$	$0 < k^2 = \dfrac{\omega^4 Q_0^2 - 2\omega^2 Q_0^2\omega_0^2 + Q_0^2\omega_0^4 + \omega^2\omega_0^2}{\omega^4 Q_0^2} < 1$ $\omega > \frac{\omega_0}{\sqrt{2}},\ Q_0^2 > \frac{\omega^2}{2\omega^2 - \omega_0^2}$
S-P	$0 = -k^2\omega^4 Q_0 + \omega^4 Q_0 - \omega^2 Q_0\omega_0^2 + Q_0\omega_0^4$ $0 = k^2\omega^2 Q_0^2 - \omega^2 Q_0^2 + Q_0^2\omega_0^2 - \omega_0^2 + \omega^2$	$Q_0^2 = \dfrac{\omega^2\omega_0^2 - \omega^4}{\omega_0^4}$ $0 < k^2 = \dfrac{(Q_0^2 - 1)(\omega^2 - \omega_0^2)}{\omega^2 Q_0^2} < 1$
P-S	$0 = k^2\omega^4 Q_0 - \omega^4 Q_0 + \omega^2 Q_0\omega_0^2 - Q_0\omega_0^4$ $0 = k^2\omega^2 Q_0^2 - \omega^2 Q_0^2 + Q_0^2\omega_0^2 - \omega_0^2 + \omega^2$	$Q_0^2 = \dfrac{\omega^2\omega_0^2 - \omega^4}{\omega_0^4}$ $0 < k^2 = \dfrac{(Q_0^2 - 1)(\omega^2 - \omega_0^2)}{\omega^2 Q_0^2} < 1$
P-P	$0 = -k^2\omega^2 Q_0^2\omega_0^2 + \omega^2 Q_0^2\omega_0^2 - 2\omega^2\omega_0^2 + \omega_0^4 - k^2\omega^4 + \omega^4$	$0 < k^2 = \dfrac{\omega^2 Q_0^2\omega_0^2 - 2\omega^2\omega_0^2 + \omega_0^4 + \omega^4}{\omega^2 Q_0^2\omega_0^2 + \omega^4} < 1$ $\omega > \dfrac{\omega_0}{\sqrt{2}}$

The values of each component using the impedance matching conditions in Table 1 and the proposed ones in Table 3 are shown in Table 4. The maximum average power calculation, $P_{av_{max}} = \frac{|E|^2}{8R_s}$, is utilized to validate the result obtained from the proposed method. Here, the resistance in power supply (R_s) is 1 Ω, and using 10 Ω for the load resistance (R_L). By selecting the input voltage magnitude $E = 2\sqrt{2}$V, the maximum possible power is normalized to 1 W. Figure 3 shows the optimum WPT power for components obtained according to Table 3, demonstrated in the "magic regime" [25]. For ease of investigation regarding whether the power transfer matches the system's ideal power, measurement intervals above 80% are colored red.

Table 4. System parameter

Topology	Impedance matching		Proposed impedance matching	
	Inductance (μH)	Capacitance (μF)	Inductance (μH)	Capacitance (μF)
S-S	L_1 =244.1	C_1 =0.476	L_1 =54.41	C_1 =1.511
	L_2 =476.6	C_2 =0.245	L_2 =544.1	C_2 =0.151
S-P	L_1 =267.0	C_1 =49.39	L_1 =3.814	C_1 =15.25
	L_2 =26.70	C_2 =488.2	L_2 =38.14	C_2 =1.525
P-S	L_1 =0.238	C_1 =488.2	L_1 =3.814	C_1 =15.25
	L_2 =238.4	C_2 =0.494	L_2 =38.14	C_2 =1.525
P-P	L_1 =53.40	C_1 =488.2	L_1 =2.025	C_1 =20.74
	L_2 =48.23	C_2 =531.3	L_2 =20.25	C_2 =2.074

The maximum power of 1 W can be achieved by using impedance-matching method calculations. In the series-series topology in Figure 3(a) the maximum power received is at a frequency of 14.75 kHz, while in the series-parallel topology in Figure 3(b) and parallel-series in Figure 3(c), it is at 1.39 and 14.75 kHz respectively. In Figure 3(d), the parallel-parallel topology reaches its maximum power value at 0.999 kHz. From these results, the first method is not able to deliver maximum power at frequencies beyond that and cannot satisfy maximum power either because the coupling coefficient shifts from the critical point of maximum power. In this condition, power cannot be maintained optimally even though the frequency is adjusted adaptively.

In contrast to the previous method, the maximum power value provided by the second method is shown in Figure 3. By using suitable components obtained from the proposed method based on impedance matching, a maximum power value of 1 W can be achieved. In Figure 3, especially the result of proposed impedance matching with the specific conditions, there are differences compared to the previous method, which are the uniformity of the maximum power value that can be performed. In the S-S configuration, it can be seen that the change in frequency from 12 to 30 kHz has a uniform maximum power value, as in Figure 3(b). The S-P and P-S topologies have the same output power characteristics and work in the frequency range 14 to 21 kHz, as in Figure 3(d) and 3(f). In Figure 3(h), the P-P has maximum power at a frequency of 14 to 30 kHz.

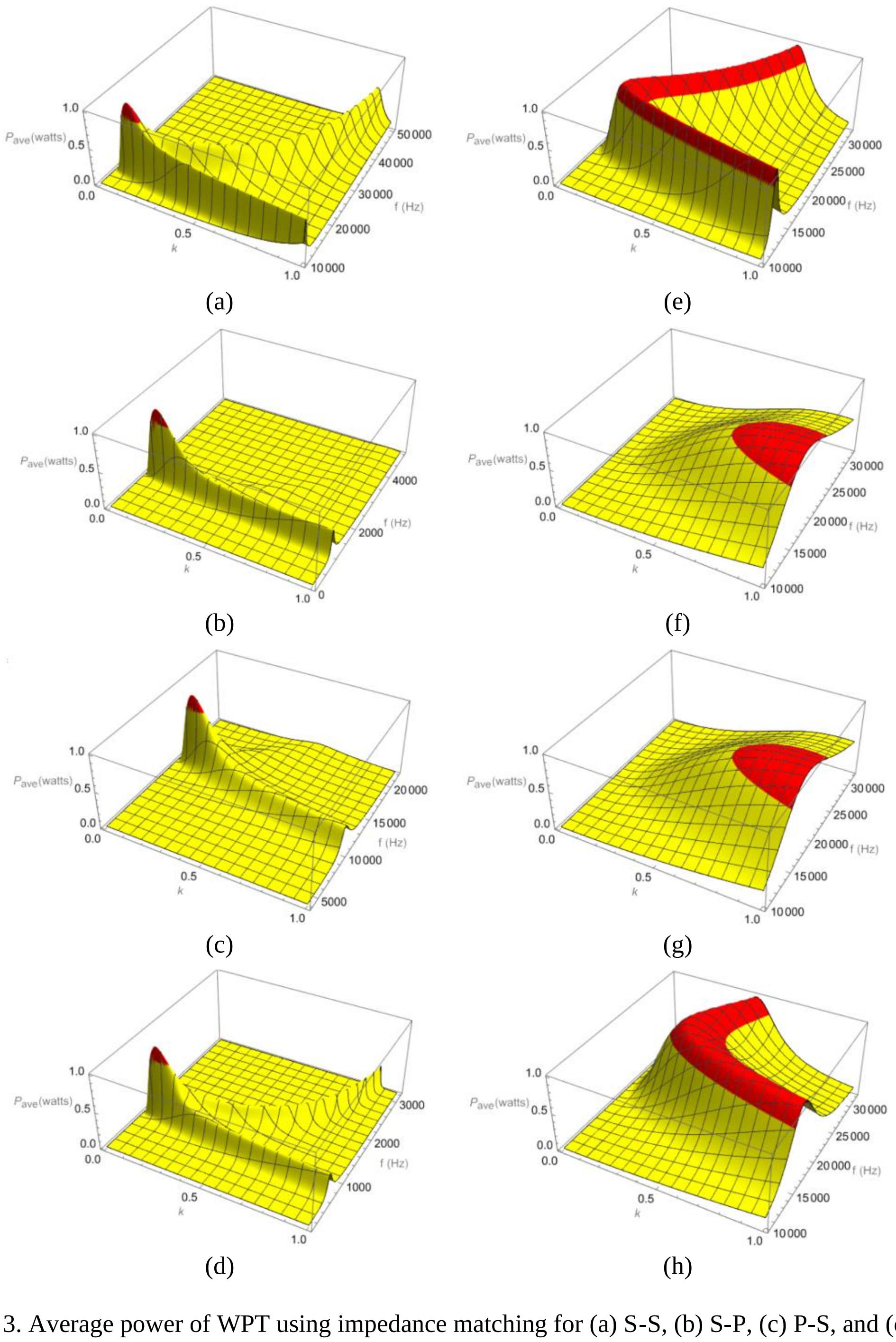

Figure 3. Average power of WPT using impedance matching for (a) S-S, (b) S-P, (c) P-S, and (d) P-P; Average power of WPT using proposed impedance matching with the specific conditions for (e) S-S, (f) S-P, (g) P-S, and (h) P-P

This scenario illustrates that if a coil misalignment occurs, the first matching condition cannot accept a significant change in the value of k because the estimate does not account for k. Therefore, it cannot compensate for the misalignment. Meanwhile, the proposed method can compensate for shifts in k values by adjusting the frequency adaptively. In terms of compensating shifts in k, the P-P has the best response because it can tolerate changes in the value of k that are more significant than other topologies. The series topology is the second-best alternative in dealing with the same problem. By selecting the frequency accurately, maximum power can still be executed even if the transmitter and receiver are misaligned.

The next issue appears when determining the component value to be used because the calculated value differs from the actual value. The previous calculation provides generated maximum power options for the S-S and P-P topologies better than the other topologies. Therefore, these two topologies are suitable for investigating further properties by adding random values to the variables L_1, L_2, C_1, and C_2 as a component tolerance and the tolerances are defined under three conditions; ± 1%, ± 5%, and ± 10%.

Figure 4 presents the responses of these two topologies with the values of f and k chosen respectively, $f = 22$ kHz and $k = 0.35$ because they produce more than 80% power for either S-S or P-P. Figure 4(a) depicts a tolerance of 1%; the working area of the P-P and S-S topologies is 95% and 85% of the maximum power, respectively. With a tolerance of 5%, the maximum power of the P-P topology achieves 70%, and the S-S topology reaches 50% of the maximum power, as shown in Figure 4(b). Using a tolerance of 10% for both topologies is the last condition to investigate the properties of these two topologies; the output power produced by the P-P topology is greater, *i.e.*, with a working area of 40% and the S-S topology's 20% of the maximum power value as depicted in Figure 4(c). Therefore, the comparison results indicate that the proposed method generates higher output power than the basic method. Additionally, the P-P topology offers the advantage that modifying the frequency simplifies reaching the maximum power transfer.

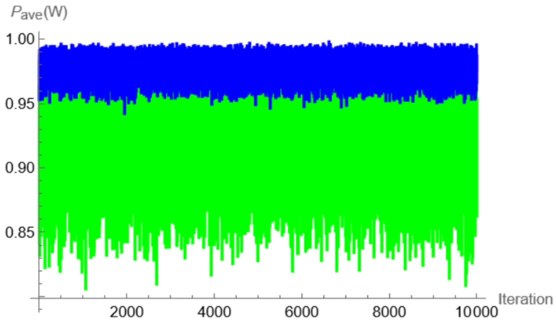

(a)

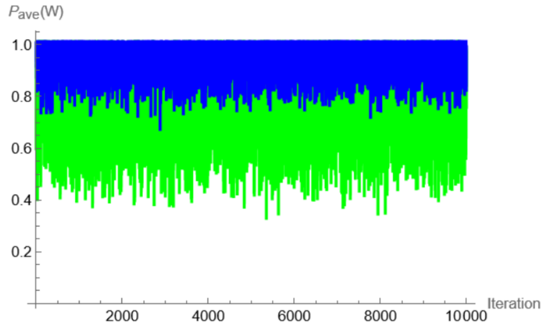

(b)

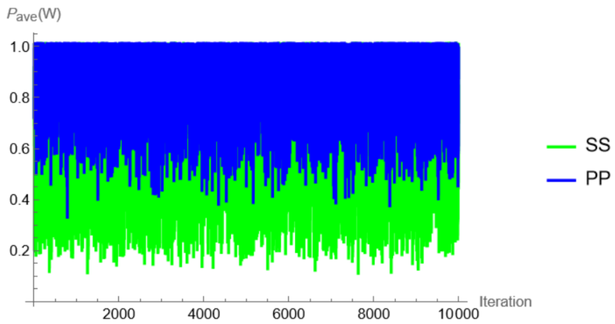

(c)

Figure 4. Comparison of the average power due to component tolerances (a) 1%, (b) 5%, and (c) 10%

This paper demonstrates several crucial points: the optimal frequency and distance of wireless power systems can be developed by considering components based on symbolic conditions. By incorporating these symbolic conditions, it becomes possible to fine-tune the system for various scenarios, ensuring maximum power transmission under different operational settings. Furthermore, using this approach, which adjusts the power transmission frequency, the distance settings have greater tolerance, which allows them to adapt effectively to dynamic environmental changes, such as inconsistent obstacles or interference.

4. CONCLUSION
By using fundamental topologies, an analytical review of WPT is presented throughout this paper. Optimization of transferred power with an impedance matching technique has been discussed. Beyond conventional impedance matching approaches, we have proposed a special condition besides impedance matching, where the maximum power can be recovered by tuning the working frequency for a variable coupling coefficient. This tuning is based on special conditions derived from the inequalities involving the coupling coefficient, frequency, and quality factor. This means that we can maximize the output power even under uncertain positions and orientations of transmitter and receiver coils. This adaptability is crucial for real-world applications were, precise alignment of coils cannot always be guaranteed.

FUNDING INFORMATION
This research was conducted without financial support from external sources.

AUTHOR CONTRIBUTIONS STATEMENT
This journal uses the Contributor Roles Taxonomy (CRediT) to recognize individual author contributions, reduce authorship disputes, and facilitate collaboration.

Name of Author	C	M	So	Va	Fo	I	R	D	O	E	Vi	Su	P	Fu
Lunde Ardhenta	✓	✓	✓	✓	✓	✓		✓	✓	✓	✓		✓	
Ichijo Hodaka	✓	✓			✓	✓		✓	✓	✓	✓	✓	✓	
Kazuya Yamaguchi						✓			✓					
Takuya Hirata						✓			✓					

C : **C**onceptualization	I : **I**nvestigation	Vi : **Vi**sualization
M : **M**ethodology	R : **R**esources	Su : **Su**pervision
So : **So**ftware	D : **D**ata Curation	P : **P**roject administration
Va : **Va**lidation	O : Writing - **O**riginal Draft	Fu : **Fu**nding acquisition
Fo : **Fo**rmal analysis	E : Writing - Review & **E**diting	

CONFLICT OF INTEREST STATEMENT
Authors state no conflict of interest.

DATA AVAILABILITY
Data availability is not applicable to this paper as no new data were created or analyzed in this study.

REFERENCES
[1] X. Lu, P. Wang, D. Niyato, D. I. Kim, and Z. Han, "Wireless charging technologies: fundamentals, standards, and network applications," *IEEE Communications Surveys and Tutorials*, vol. 18, no. 2, pp. 1413–1452, 2016, doi: 10.1109/COMST.2015.2499783.
[2] H. Barth, M. Jung, M. Braun, and B. Schmuelling, "Concept evaluation of an inductive charging system for electric vehicles," in *3rd European Conference SmartGrids and E-Mobility*, 2011.
[3] Y. Zhang *et al.*, "Misalignment-tolerant dual-transmitter electric vehicle wireless charging system with reconfigurable topologies," *IEEE Transactions on Power Electronics*, vol. 37, no. 8, pp. 8816–8819, Aug. 2022, doi: 10.1109/TPEL.2022.3160868.
[4] V. Sari, "Design and implementation of a wireless power transfer system for electric vehicles," *World Electric Vehicle Journal*, vol. 15, no. 3, Mar. 2024, doi: 10.3390/wevj15030110.
[5] C. H. Lee, G. Jung, K. Al Hosani, B. Song, D. K. Seo, and D. Cho, "Wireless power transfer system for an autonomous electric vehicle," in *2020 IEEE Wireless Power Transfer Conference, WPTC 2020*, Nov. 2020, pp. 467–470. doi: 10.1109/WPTC48563.2020.9295631.
[6] J. Minguillon *et al.*, "Powering electronic implants by high frequency volume conduction: In human validation," *IEEE Transactions on Biomedical Engineering*, vol. 70, no. 2, pp. 659–670, Feb. 2023, doi: 10.1109/TBME.2022.3200409.
[7] G. Monti, G. R. De Giovanni, M. De Liso, M. Pascali, and L. Tarricone, "Wireless power transfer strategies for medical implants: Focus on robustness and EM compatibility," *IEEE Microwave Magazine*, vol. 22, no. 9, pp. 28–41, Sep. 2021, doi: 10.1109/MMM.2021.3086315.
[8] W. Lee and Y. K. Yoon, "High efficiency metamaterial-based multi-scale wireless power transfer for smart home applications," in *IEEE MTT-S International Microwave Symposium Digest*, Jun. 2021, vol. 2021-June, pp. 62–65. doi: 10.1109/IMS19712.2021.9574860.
[9] Z. Zhang, A. Georgiadis, and C. Cecati, "Wireless power transfer for smart industrial and home applications," *IEEE Transactions on Industrial Electronics*, vol. 66, no. 5, pp. 3959–3962, May 2018, doi: 10.1109/TIE.2018.2884307.

[10] J. Stillig and N. Parspour, “Classification of WPT systems: Categorization, differentiation and overview of industrial wireless power transfer systems,” in *9th IEEE International Conference on Power Electronics, Drives and Energy Systems, PEDES 2020*, Dec. 2020, pp. 1–6. doi: 10.1109/PEDES49360.2020.9379884.
[11] Z. Zhang, H. Pang, A. Georgiadis, and C. Cecati, “Wireless power transfer - an overview,” *IEEE Transactions on Industrial Electronics*, vol. 66, no. 2, pp. 1044–1058, Feb. 2019, doi: 10.1109/TIE.2018.2835378.
[12] W. Zhang and C. C. Mi, “Compensation topologies of high-power wireless power transfer systems,” *IEEE Transactions on Vehicular Technology*, vol. 65, no. 6, pp. 4768–4778, Jun. 2016, doi: 10.1109/TVT.2015.2454292.
[13] M. Yilmaz and P. T. Krein, “Review of battery charger topologies, charging power levels, and infrastructure for plug-in electric and hybrid vehicles,” *IEEE Transactions on Power Electronics*, vol. 28, no. 5, pp. 2151–2169, May 2013, doi: 10.1109/TPEL.2012.2212917.
[14] X. Shu, G. Wu, and Y. Jiang, “Comparative analysis of SS, SP, PP and PS topologies for magnetic coupled wireless power transfer system composed of the negative resistor,” *Energies*, vol. 16, no. 21, p. 7336, Oct. 2023, doi: 10.3390/en16217336.
[15] A. Laha, A. Kalathy, M. Pahlevani, and P. Jain, “A comprehensive review on wireless power transfer systems for charging portable electronics,” *Eng*, vol. 4, no. 2, pp. 1023–1057, Apr. 2023, doi: 10.3390/eng4020061.
[16] V. Shevchenko, O. Husev, R. Strzelecki, B. Pakhaliuk, N. Poliakov, and N. Strzelecka, “Compensation topologies in IPT systems: Standards, requirements, classification, analysis, comparison and application,” *IEEE Access*, vol. 7, pp. 120559–120580, 2019, doi: 10.1109/ACCESS.2019.2937891.
[17] X. Dai, Y. Huang, and Y. Li, “Topology comparison and selection of wireless power transfer system and parameter optimization for high voltage gain,” in *2017 IEEE PELS Workshop on Emerging Technologies: Wireless Power Transfer, WoW 2017*, May 2017, pp. 1–5. doi: 10.1109/WoW.2017.7959414.
[18] A. Sagar, M. Bertoluzzo, and A. Kumar, “Analysis and comprehensive comparison of wireless power transfer system using SS and SP topology for electric vehicle charging,” in *2023 International Conference on Computational Intelligence, Communication Technology and Networking, CICTN 2023*, Apr. 2023, pp. 235–240. doi: 10.1109/CICTN57981.2023.10140761.
[19] H. Movagharnejad and A. Mertens, “Design metrics of compensation methods for contactless charging of electric vehicles,” in *2017 19th European Conference on Power Electronics and Applications, EPE 2017 ECCE Europe*, Sep. 2017, vol. 2017-Janua, p. P.1-P.10. doi: 10.23919/EPE17ECCEEurope.2017.8099403.
[20] K. Detka and K. Górecki, “Wireless power transfer—a review,” *Energies*, vol. 15, no. 19, p. 7236, Oct. 2022, doi: 10.3390/en15197236.
[21] A. Mahesh, B. Chokkalingam, and L. Mihet-Popa, “Inductive wireless power transfer charging for electric vehicles - a review,” *IEEE Access*, vol. 9, pp. 137667–137713, 2021, doi: 10.1109/ACCESS.2021.3116678.
[22] M. Rehman, P. Nallagownden, and Z. Baharudin, “Efficiency investigation of SS and SP compensation topologies for wireless power transfer,” *International Journal of Power Electronics and Drive Systems (IJPEDS)*, vol. 10, no. 4, pp. 2157–2164, Dec. 2019, doi: 10.11591/ijpeds.v10.i4.pp2157-2164.
[23] C. Sen Wang, G. A. Covic, and O. H. Stielau, “Power transfer capability and bifurcation phenomena of loosely coupled inductive power transfer systems,” *IEEE Transactions on Industrial Electronics*, vol. 51, no. 1, pp. 148–157, Feb. 2004, doi: 10.1109/TIE.2003.822038.
[24] M. Venkatesan *et al.*, “A review of compensation topologies and control techniques of bidirectional wireless power transfer systems for electric vehicle applications,” *Energies*, vol. 15, no. 20, p. 7816, Oct. 2022, doi: 10.3390/en15207816.
[25] A. P. Sample, D. A. Meyer, and J. R. Smith, “Analysis, experimental results, and range adaptation of magnetically coupled resonators for wireless power transfer,” *IEEE Transactions on Industrial Electronics*, vol. 58, no. 2, pp. 544–554, Feb. 2011, doi: 10.1109/TIE.2010.2046002.

BIOGRAPHIES OF AUTHORS

Lunde Ardhenta received the bachelor degree in Department of Electrical Engineering from the Universitas Brawijaya, Malang, Indonesia, in 2011 and the master degree in the same major from the National Chiayi University, Chiayi, Taiwan, in 2015. He is currently pursuing a Ph.D. in the Department of Materials and Informatics, Interdisciplinary Graduate School of Agriculture and Engineering, University of Miyazaki. Additionally, he serves as a faculty member in the Department of Electrical Engineering at Universitas Brawijaya, Malang, Indonesia. He can be contacted at email: nc23005@student.miyazaki-u.ac.jp.

Ichijo Hodaka graduated from the Department of Aeronautical Engineering, Faculty of Engineering at Nagoya University in March 1992. He completed his master's degree in aeronautical engineering from the Graduate School of Engineering at Nagoya University in March 1994 and left the doctoral program in aerospace engineering at the same institution in June 1997. In November 1999, he was awarded a Doctor of Engineering from Nagoya University for his dissertation on control system design based on dissipative systems theory. He began his academic career as a research associate in the Graduate School of Engineering at Nagoya University in June 1997, was promoted to lecturer in October 2001, and then took a position as an associate professor in the Department of Electrical and Electronic Engineering at the University of Miyazaki in October 2007. He was promoted to professor in the School of Engineering at the University of Miyazaki in April 2011. Professor Hodaka's research interests include wireless power transmission and renewable energy systems by applying control theory. He can be contacted at email: hijhodaka@cc.miyazaki-u.ac.jp.

Kazuya Yamaguchi pursued a degree at the University of Miyazaki from 2007 to 2016 in the Department of Electrical and Electronic Engineering. In his study, he developed a method for determining efficient frequencies in wireless power transfer. He is currently joining the National Institute of Technology, Nara College, to conduct further research. Now, he lectures on electric circuits and electromagnetics and conducts electrical and electronic engineering experiments. He can be contacted at email: k-yamaguchi@ctrl.nara-k.ac.jp.

Takuya Hirata earned his Ph.D. from the University of Miyazaki in 2017. He is currently working at the University of Miyazaki as an assistant professor in the Department of Electrical and Electronic Engineering. His research focuses on wireless power transmission and photovoltaic systems. He can be contacted at email: hirata.takuya.p2@cc.miyazaki-u.ac.jp.